

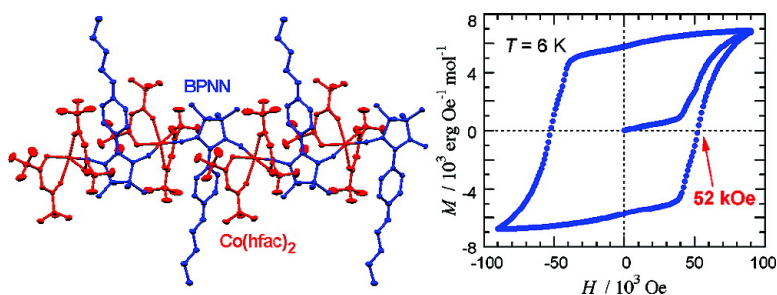
Communication

Giant Coercivity in a One-Dimensional Cobalt-Radical Coordination Magnet

Norio Ishii, Yoshitomo Okamura, Susumu Chiba, Takashi Nogami, and Takayuki Ishida

J. Am. Chem. Soc., **2008**, 130 (1), 24-25 • DOI: 10.1021/ja077666e

Downloaded from <http://pubs.acs.org> on February 8, 2009



More About This Article

Additional resources and features associated with this article are available within the HTML version:

- Supporting Information
- Links to the 5 articles that cite this article, as of the time of this article download
- Access to high resolution figures
- Links to articles and content related to this article
- Copyright permission to reproduce figures and/or text from this article

[View the Full Text HTML](#)

Giant Coercivity in a One-Dimensional Cobalt-Radical Coordination Magnet

Norio Ishii,[†] Yoshitomo Okamura,[†] Susumu Chiba,[†] Takashi Nogami,[†] and Takayuki Ishida^{*,†,‡}

Department of Applied Physics and Chemistry and Course of Coherent Optical Science, The University of Electro-Communications, Chofu, Tokyo 182-8585, Japan

Received October 4, 2007; E-mail: ishi@pc.uec.ac.jp

There have been a number of examples of low-dimensional complexes containing nitronyl nitroxide (NN) radicals with metal hfac salts, in pursuit of metal-radical hybrid magnets¹ (the systematic name of NN is 4,4,5,5-tetramethylimidazolin-1-oxyl 3-oxide). Since the discovery of the first single-chain magnet (SCM) [Co(hfac)₂·AnNN] by Gatteschi et al.² (Scheme 1 with R = CH₃), several derivatives containing smaller ligands³ and 4f-metal ions⁴ and other systems^{5,6} have been extensively investigated toward novel SCMs. Intermolecular interaction among the single-molecule magnets (SMMs) has been discussed for a dimer of the [Mn₄]-based SMM.⁷ Similarly, there seems to be a chance to introduce interchain interaction to SCM systems because various [M^{II}(hfac)₂·RNN] chains exhibited magnetic ordering.¹ We found interplay between SCM and bulk characters and considerably large coercivity in [Co(hfac)₂·BPNN] (**1**; BPNN = *p*-butoxyphenyl-NN). Actually, **1** can be regarded as one of the hardest magnets ever reported.

Complexation of Co(hfac)₂ with BPNN gave **1** as bluish purple needles (see Supporting Information), according to the conventional method.¹ As X-ray crystallographic analysis on **1** revealed, there are two independent units in a monoclinic unit cell of **1**, each of which is arranged to form a metal-radical alternating chain running along the crystallographic *b*-axis (Figure 1S in Supporting Information). The geometries are similar to each other, and the magnetic properties imply the sum of the two kinds of chains. The radical oxygen atoms are located in a *cis* manner around the Co ions, and the nearest intrachain Co–Co distances are 7.4659(4) and 7.4301(4) Å. Interchain Co–Co distances are 10.3 Å and larger. The bulky butoxy group might affect the crystal field and magnetic anisotropy of the Co ions. The helical pitch is also changed: 2₁ symmetry for **1** versus 3₁ for the methyl analogue.²

We measured the static molar magnetic susceptibility (χ_{mol} on the repeating unit basis) on a polycrystalline **1** (Figure 2S in Supporting Information). The temperature dependence of $\chi_{\text{mol}}T$ showed an upsurge on cooling, clearly indicating the ferrimagnetic spin alignment within a chain, as usually observed for [Co(hfac)₂·RNN]-type polymers.^{1–3}

As Figure 1a shows, the FCM of **1** gradually increases around 80 K and reaches a plateau below ca. 45 K. On the other hand, the RM starts to decay rapidly at 10 K, not 45 K, on warming, and the ZFCM curve starts to increase at 10 K. We examined the magnetic anisotropy of **1**. Single-crystal FCM measurements on **1** (the inset of Figure 1a) revealed that the magnetic hard axis corresponded to the chain direction.

We first examined the anomaly around 10 K (for the magnetic behavior around 45 K, see below). Figure 1b shows a remarkable frequency dependence of the ac magnetic susceptibility on **1**. A half-circle was drawn in the Cole–Cole plot (the inset). We obtained $\alpha = 0.251$, indicating the presence of a single relaxation process.⁸ The frequency dependence of peak temperature in χ' , ϕ

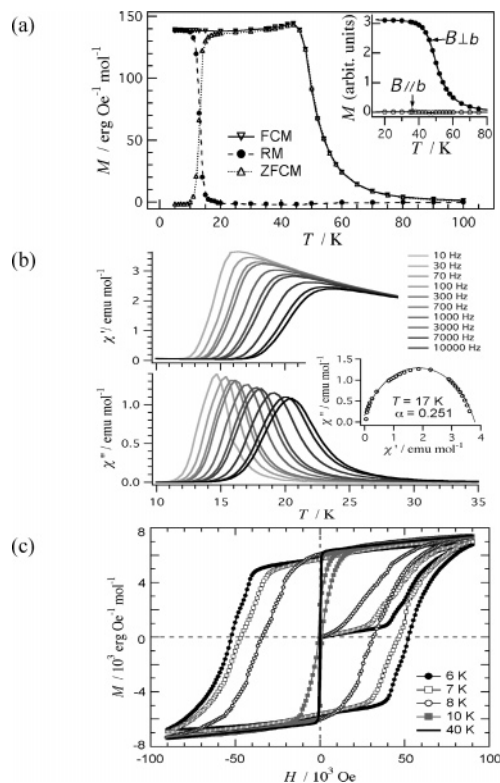
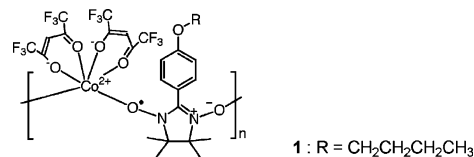


Figure 1. (a) FCM (field-cooled magnetization), RM (remnant magnetization), and ZFCM (zero-field-cooled magnetization) for randomly oriented polycrystalline **1** with the applied field of 5 Oe. Inset: FCM curves for single crystals of **1** with the field of 100 Oe applied in the directions parallel and perpendicular to the *b*-axis. (b) In-phase and out-of-phase ac magnetic susceptibilities, χ' and χ'' , respectively, of polycrystalline **1** as a function of temperature and frequency. The ac field amplitude was 5 Oe. Inset: the Cole–Cole plot at 17 K. (c) Hysteresis loops of polycrystalline **1** measured at 6, 7, 8, 10, and 40 K.

Scheme 1



$= (\Delta T_p/T_p)/\Delta(\log \omega)$, was 0.12, which excludes the possibility of a spin-glass ($0.01 < \phi < 0.08$).⁹ The relaxation rate ($1/\tau$) is equal to the frequency of the applied ac field ($2\pi\nu$) at the temperature of the maximum of χ'' . We can analyze the energy barrier (E_a) of the magnetization reorientation based on an Arrhenius-type equation,^{5,9} $\ln(2\pi\nu) = -\ln(\tau_0) - E_a/k_B T$, giving $E_a/k_B = 350(6)$ K and $\tau_0 = 6.8 \times 10^{-13}$ s. The temperature at which the dynamic process is sufficiently slow as $\nu = 10^{-4}$ Hz (i.e., τ becomes hours) is 10 K, in good agreement with the RM and ZFCM relaxation (Figure 1a).

[†] Department of Applied Physics and Chemistry.

[‡] Course of Coherent Optical Science.

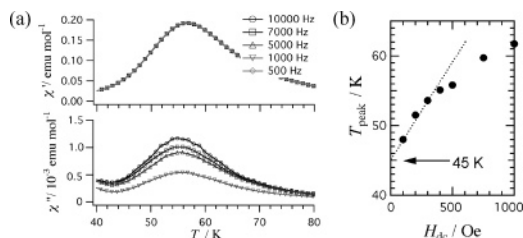


Figure 2. (a) Ac magnetic susceptibilities of **1** as a function of temperature, with the static field (H_{dc}) of 500 Oe. The ac field amplitude was 5 Oe. The χ' curves showed practically the same profiles regardless of frequency. (b) The peak temperature as a function of H_{dc} .

The E_a value of **1** is much larger than those of known SCMs^{2–6} ($E_a/k_B = 154(2) \text{ K}^2$ or $72(1) \text{ K}^5$ for instance).

The magnetization curves of **1** showed an almost saturated value of $8 \times 10^3 \text{ erg Oe}^{-1} \text{ mol}^{-1}$ at 9 T (Figure 1c), which agrees with a residual moment from the ferrimagnetically correlated Co and NN spins. Below 10 K, **1** behaved as a very hard magnet showing a large hysteresis loop. A coercive field (H_C) was 52 kOe at 6 K. The magnetic anisotropy of **1** was confirmed by using a single crystal (Figure 3S in Supporting Information). On the other hand, the magnetization process turned typical of a soft magnet above 10 K; H_C drastically became small, owing to the fast relaxation as described above.

We measured the ac susceptibilities of polycrystalline **1** around 45 K with a static bias field (H_{dc}). A broad peak appeared at 56 K at $H_{dc} = 500 \text{ Oe}$, and the peak temperature was frequency-independent (Figure 2a). Such an almost null ϕ parameter on this peak suggests the ferromagnetic (or weak ferromagnetic) order.⁹ The larger H_{dc} gave the higher peaking temperature (Figure 2b), in agreement with ferromagnetic coupling of the chains. A critical temperature (T_C) is estimated to be 45 K from extrapolation to zero H_{dc} . The FCM curve showed a small cusp at 45 K (Figure 1a).

The apparent “blocking” behavior took place after **1** became a soft magnet, in sharp contrast with the bridged $[\text{Mn}_4]$ SMMs, in which the discrete magnetic moments are blocked first and then a long-range order starts.¹⁰ How can we explain the present results? The term “glass” is usually used for the frozen spin systems consisting of single ions or molecules, but Coronado et al. reported the glassy behavior for motion of the magnetic domain wall in the hexacyanoferrate(III)-based layered magnet.¹¹ Similar behavior was recently observed in a cobalt(II)-biradical chain.¹² Miller et al. also reported the glassy behavior of the magnetically ordered metal-radical compound with large H_C .¹³

The macroscopic domain wall movement requires reorientation at an individual chain within a width of the wall. As for one chain, we assume that a “kink” between two opposite magnetizations moves along the chain. This model is consistent with the observed singularity of a relaxation process and its activation energy is related with the nearest-neighbor exchange interaction, as originally proposed by Glauber.¹⁴ In the magnetically ordered state, E_a is more enhanced than that of genuine SCMs because the magnetization reorientation occurs in a collective manner and the pinning effect due to the lattice defect is usually present. Thus, the slow dynamics of **1** below 10 K (freezing temperature, T_f) can be attributed to a glass of the domain wall motion.

One may point out the possibility of a “finite-size effect” on short-range ordered SCMs since a similar χ' peak was reported for $[\text{Co}(\text{hfac})_2 \cdot \text{AnNN}]$.¹⁵ However, the present situation seems somewhat different because we found the cusp in the FCM, the very large E_a , and the typical soft ferromagnet behavior at 40 K just below T_C (Figure 1c). In addition, the axial anisotropy along the chain was characterized for $[\text{Co}(\text{hfac})_2 \cdot \text{AnNN}]$,² while the magnetic

easy axis lies perpendicular to the chain direction for **1**. The latter case favors ferromagnetic coupling among the magnetic chains in a dipolar manner.¹⁶ We could observe no heat capacity peak due to magnetic phase transition so far. It may be because a major fraction of the magnetic entropy of the ferrimagnetic chains is broadly present above T_C (or T_f), as supported by the short-range order accompanied by a very wide FCM slope up to ca. 80 K (Figure 1a). We can explain the state in this slope region in terms of a model of ferromagnetic islands in a paramagnetic sea. Below T_C , the initial steep upsurge of the magnetization at 40 K implies that the whole fraction of **1** forms ferromagnetic domains. Since the magnetic state at $T_f < T \leq T_C$ exhibits such a bulk property, we empirically call this state as a soft-magnet phase. A long-range order is likely to occur before it behaves as a hard magnet, and the investigation on ordering is now in progress.

In summary, we can draw the phase diagram of **1** as follows: a hard magnet in $T \leq T_f$ and a soft magnet at $T_f < T \leq T_C$. A magnetization jump at zero field (above T_f in Figure 1c) may give rise to loss of stored information and thus difficulty in future application. However, magnetically correlated SCMs of **1** possessed a very high effective E_a below T_f . Introduction of an interchain interaction can improve magnetic hardness and avoid magnetization loss at zero field. Actually, the H_C was 52 kOe (4.1 MA m^{-1}) at 6 K (Figure 1c), which is much larger than those of the molecule-based $[\text{MnTBrPP}][\text{TCNE}] \cdot 2(\text{CH}_2\text{Cl}_2)$ (27.8 kOe at 2 K as the largest value before this work)¹³ and even commercial permanent magnets SmCo_5 (44 kOe at room temperature) and $\text{Nd}_2\text{Fe}_{14}\text{B}$ (19 kOe at room temperature).¹⁷ To the best of our knowledge, **1** enjoys being a record holder of the largest coercive field among hard magnets ever known.

Supporting Information Available: Figures 1S–3S, experimental details, and the CIF file of **1**. This material is available free of charge via the Internet at <http://pubs.acs.org>.

References

- (1) (a) Caneschi, A.; Gatteschi, D.; Sessoli, R. *Acc. Chem. Res.* **1989**, *22*, 392. (b) Caneschi, A.; Gatteschi, D.; Rey, P. *Prog. Inorg. Chem.* **1991**, *39*, 33.
- (2) Caneschi, A.; Gatteschi, D.; Lalioti, N.; Sangregorio, C.; Sessoli, R.; Venturi, G.; Vindigni, A.; Rettori, A.; Pini, M. G.; Novak, M. A. *Angew. Chem., Int. Ed.* **2001**, *40*, 1760.
- (3) Ishii, N.; Ishida, T.; Nogami, T. *Inorg. Chem.* **2006**, *45*, 3837.
- (4) (a) Bogani, L.; Sangregorio, C.; Sessoli, R.; Gatteschi, D. *Angew. Chem., Int. Ed.* **2005**, *44*, 5817. (b) Bernot, K.; Bogani, L.; Caneschi, A.; Gatteschi, D.; Sessoli, R. *J. Am. Chem. Soc.* **2006**, *128*, 7947.
- (5) Clérac, R.; Miyasaka, H.; Yamashita, M.; Coulon, C. *J. Am. Chem. Soc.* **2002**, *124*, 12837.
- (6) Miyasaka, H.; Madanbashi, T.; Sugimoto, K.; Nakazawa, Y.; Wernsdorfer, W.; Sugiura, K.-i.; Yamashita, M.; Coulon, C.; Clérac, R. *Chem.—Eur. J.* **2006**, *12*, 7028 and references cited therein.
- (7) Wernsdorfer, W.; Aliaga-Alcalde, N.; Hendrickson, D. N.; Christou, G. *Nature* **2002**, *416*, 406.
- (8) Gatteschi, D.; Sessoli, R. *Angew. Chem., Int. Ed.* **2003**, *42*, 268.
- (9) (a) Gatteschi, D.; Sessoli, R.; Villain, J. *Molecular Nanomagnets*; Oxford University Press: New York, 2006; pp 69–75. (b) Hibbs, W.; Rittenberg, D. K.; Sugiura, K.-i.; Burkhart, B. M.; Morin, B. G.; Arif, A. M.; Liable-Sands, L.; Rheingold, A. L.; Sundaralingam, M.; Epstein, A. J.; Miller, J. S. *Inorg. Chem.* **2001**, *40*, 1915.
- (10) Miyasaka, H.; Nakata, K.; Lecren, L.; Coulon, C.; Nakazawa, Y.; Fujisaki, T.; Sugiura, K.-i.; Yamashita, M.; Clérac, R. *J. Am. Chem. Soc.* **2006**, *128*, 3770.
- (11) Coronado, E.; Gómez-García, C. J.; Nuez, A.; Romero, F. M.; Waerenborgh, C. J. *Chem. Mater.* **2006**, *18*, 2670.
- (12) Numata, Y.; Inoue, K.; Baranov, N.; Kurmoo, M.; Kikuchi, K. *J. Am. Chem. Soc.* **2007**, *129*, 9902.
- (13) (a) Rittenberg, D. K.; Sugiura, K.-i.; Sakata, Y.; Mikami, S.; Epstein, A. J.; Miller, J. S. *Adv. Mater.* **2000**, *12*, 126. (b) Epstein, A. J. *MRS Bull.* **2000**, *25*, 33.
- (14) Glauber, R. J. *J. Math. Phys.* **1963**, *4*, 294.
- (15) Bogani, L.; Sessoli, R.; Pini, M. G.; Rettori, A.; Novak, M. A.; Rosa, P.; Massi, M.; Fedi, M. E.; Giuntini, L.; Caneschi, A.; Gatteschi, D. *Phys. Rev. B* **2005**, *72*, 064406.
- (16) Wynn, C. M.; Girtu, M. A.; Brinckerhoff, W. B.; Sugiura, K.-i.; Miller, J. S.; Epstein, A. J. *Chem. Mater.* **1997**, *9*, 2156.
- (17) Fildler, J.; Schrefl, T.; Hoefinger, S.; Hajduga, M. *J. Phys.: Condens. Matter.* **2004**, *16*, S455.

JA077666E